Available online at www.sciencedirect.com
SCIENCE DIRECT®
PERGAMON
Acta Astronautica 59 (2006) 367–380
ACTA ASTRONAUTICA
www.elsevier.com/locate/actaastro

Transfers between the Earth–Moon and Sun–Earth systems using manifolds and transit orbits

Kathleen C. Howell*, Masaki Kakoi

Purdue University, West Lafayette, Indiana, USA

Available online 12 May 2006

Abstract

The L_1 and L_2 libration points have been proposed as gateways granting inexpensive access to interplanetary space. The lunar libration points, in conjunction with the collinear libration points in the Sun–Earth system, may also become primary hubs for future human activities in the Earth's neighborhood. The associated manifold tubes have been introduced by a number of researchers as the basis for design strategies to produce trajectories that shift between different systems. Intersections may ultimately be sought between many tubes from many different libration point orbits in each system; the complexity forces a new look at the computations. Individual transfers between three-body systems have been the focus of some recent investigations. This paper presents an approach to solve the general problem for transfers between the Earth–Moon system (lunar orbits and/or lunar libration point orbits) and Sun–Earth/Moon L_2 libration point orbits. The solutions are transitioned to the full ephemeris models with additional perturbations and the transfers can be determined for various lunar phases. The solution process also seeks the particular Lissajous trajectory in each system to accomplish the transfer at a low cost. Some results are presented for various types of transfer problems.

1. Introduction

After numerous successful missions involving Sun–Earth libration point orbits, the design potential in multi-body regimes has generated great interest. For example, the lunar libration points, in conjunction with the collinear libration points in the Sun–Earth system, could become primary hubs for future human activities in the Earth's neighborhood [1]. Large astronomical observatories will likely be located near the Sun–Earth L_2 point requiring human servicing and repair [2]. The Earth–Moon L_1 libration point is suggested as a possible staging node for missions to the Sun–Earth L_2 point as well as the Moon, Mars, and the rest of the solar system. Thus, the L_1 and L_2 libration points have also been proposed as gateways granting inexpensive access to interplanetary space [3]. Libration point orbits in other three-body systems might also facilitate understanding of the structure of the solar system and the design of low energy transfers throughout interplanetary space [4–6]. As the possibilities expand, it becomes essential to further develop efficient numerical tools for analysis and design in such multi-body regimes. Halo orbits and invariant manifolds are now well-known dynamical structures in this region of space and have been employed as tools to design various types of transfers and spacecraft trajectories. But, the complexity is increasing. For near-term plans in the Earth's neighborhood, numerous proposals for infrastructure as well as

* Corresponding author. Tel.: +1 317 494 5786; fax: +1 317 494 0307.
E-mail addresses: howell@ecn.purdue.edu (K.C. Howell), kakoi@purdue.edu (M. Kakoi).

0094-5765/$ - see front matter © 2006 Elsevier Ltd. All rights reserved.
doi:10.1016/j.actaastro.2006.02.010

exploratory and scientific missions involve spacecraft moving freely throughout the local space where the Sun, Earth, and Moon all contribute as significant gravitational influences. Essentially a four-body problem, it can also be envisioned as two overlapping three-body problems, i.e., the Sun–Earth and Earth–Moon systems. The application of the periodic orbit and invariant manifold structure is a natural approach to support the design process in such problems. To move freely between the regions dominated by each three-body system requires a system-to-system transfer.

With the huge expansion in numerical capabilities over the last few decades, insight into the dynamical foundations of the three-body problem has increased significantly. Successful exploitation of periodic halo orbits and quasi-periodic Lissajous trajectories for spacecraft mission design have fueled further study. The flow toward and away from the periodic orbits is represented by the stable and unstable invariant manifolds. The trajectories that comprise the manifolds corresponding to a single halo orbit are infinite in number and reside on the surface of a tube. A family of halo orbits actually exists near any collinear libration orbit, each orbit with a tube corresponding to its invariant manifolds. The design space, then, includes not just a single tube corresponding to the invariant manifolds of one halo orbit; rather, it becomes a volume consisting of many tubes. If the stable/unstable tubes represent flow toward and away from the periodic orbit in a given three-body system, they can be used to "overlap" one three-body system with another and create system-to-system transfers.

Koon et al. [7–9] introduce the manifold tubes as the basis for a design strategy to move between systems and discuss it in detail for a low cost transfer between the Earth–Moon and Sun–Earth systems. It is also examined in the Jovian system [10]. Thus, transfers between three-body systems can be modeled in terms of the intersection of two tubes—one from each system. A maneuver at or near an intersection point will shift the vehicle from one tube to the other. However, the search for an intersection between two tubes is numerically intense. Without an analytical representation for the invariant manifolds, this simple task can become quite challenging. The usefulness of the Poincaré section to examine the intersection between two tubes from different systems and successfully compute a transfer has been demonstrated in the two-dimensional (2D) problem [7,8]. First, the Jacobi constant in the planar circular restricted three-body problem (CR3BP) reduces the four-dimensional phase space by one. Using a Poincaré section to examine a slice of the reduced phase space results in a 2D image and, thus, in the planar problem, the solution space can be visualized. Still, the complexity remains when the particular halo orbits in each system are not known a priori. Then, the design space becomes a multi-dimensional volume consisting of many manifold tubes. In the planar CR3BP, the tube is also a separatrix, i.e., it separates two of the four types of motion: transit orbits and nontransit orbits [7–9]. The transit orbits are those trajectories that pass inside the manifold tubes; the tubes can then be considered as the boundary for transit flow through the pathway, in the vicinity of the collinear libration points, that connects the interior and exterior regions in the CR3BP. Nontransit orbits remain outside of the tubes and do not move between one region and another. The attempt to compute low cost transfers using transit orbits in 2D has also been successful [7–9].

The system-to-system three-dimensional (3D) transfer problem has also been studied [11,12]. The transition from 2D to 3D adds a significant amount of complexity, however. The first step is to expand the concept of Poincaré sections to the spatial problem. Such an approach has been accomplished for an Earth-to-Moon transfer in the CR3BP [11]. It is also a considerable challenge to build a reasonable 3D model that can be used for an initial design such that it is easily shifted to the ephemeris model. The result in Gómez et al. [11] is eventually computed in a true four-body bi-circular model. An alternative strategy for using manifold approximations to transition to the ephemeris model is also successful [13]. This latter approach allows for a volume of manifolds in the design space and determines a particular manifold and, therefore, a Lissajous trajectory in the ephemeris model. The result minimizes the cost for a system-to-system transfer in the Sun–Earth–Moon space. Yet, an initial reference trajectory that meets some set of general specifications for a particular type of transfer is still required. This study offers a methodology for preliminary transfer design between the Earth–Moon system (lunar orbits and/or lunar libration point orbits) and Sun–Earth/Moon L_2 libration point orbits, without perfect knowledge of the departure and/or arrival orbits. It is based on the availability of families of periodic orbits and the invariant manifolds within each system. Originating with the circular restricted problem, the solution is generated by overlapping the two different three-body systems—assuming that the two systems are in different planes. Halo-to-halo transfers, as well as halo-to-Moon transfers, have been computed by exploiting the invariant manifolds and the concept of transit

orbits. Results are transitioned into the ephemeris model.

2. Background

In the vicinity of the Earth and the Moon, the Sun's gravity can also have a significant influence on spacecraft trajectories. Thus, design in the Sun–Earth–Moon system is actually a four-body problem. Without an analytical solution and a solid map of the four-body space, the design problem is constructed as overlapping three-body problems. Some basic definitions are useful to facilitate the overlap of two three-body systems.

2.1. Circular restricted three-body problem

The Sun–Earth–Moon system is modeled in terms of two circular restricted three-body problems, the Earth–Moon system and the Sun–Earth system. In the Earth–Moon system, the origin is shifted to the Earth. This system can be modeled within the Sun–Earth system to capture the complete four-body motion. Of course, the lunar orbit is not actually in the Sun–Earth plane. To model this out-of-plane reality, a body-two 3-1-3 Euler angle sequence is useful. The schematics appear in Fig. 1. In the figure, the orthonormal vector triad $[X, Y, Z]$ defines the Sun–Earth rotating frame, and the orthonormal triad $[x, y, z]$ represents the basis vectors in the Earth–Moon rotating frame. The origins of both frames are located at the Earth. The Moon is defined to be on the x-axis. Three angles, α, i, and β appear in the figure. When all angles are zero, the Earth–Moon and the Sun–Earth rotating frames are the same. In the 3-1-3 angle sequence, the first angle α defines the position of the lunar line of nodes with respect to the X-axis. The second angle is i, the inclination angle, and is fixed to be 5° in this model. The third angle, β, positions the Moon in its orbit with respect to the line of nodes. This model is simple but allows information available from the CR3BP, such as libration points, halo orbits, and invariant manifolds, to be accessed. Of course, the angle sequence translates into timing information in the ephemeris model and, if the solution is sufficiently accurate, a transition to the full model.

2.2. Sun–Earth and Earth–Moon manifolds

It is possible to depart a Sun–Earth halo orbit anytime using unstable manifolds, for essentially no departure cost. However, globalization of the unstable manifolds reveals the unstable manifold tube and the limited regions of space that can be accessed. The tube may deliver a vehicle to a wide variety of locations depending on the particular halo orbit with which the tube is associated and the specific trajectory that is exploited. Only certain manifolds might deliver a spacecraft to the desired location, and/or no manifolds may be available that reach the desired location in a reasonable time. The basis for a system-to-system transfer is a requirement that the Sun–Earth manifolds intersect the Earth–Moon manifolds. An example of a Sun–Earth unstable manifold tube appears in Fig. 2. These manifolds are associated with a halo orbit defined by an in-plane excursion amplitude of $Ay = 699,000$ km and an out-of-plane amplitude $Az = 200,000$ km. It is obvious that some of the manifolds pass very close to the Earth. These manifolds do not generally yield productive intersections with

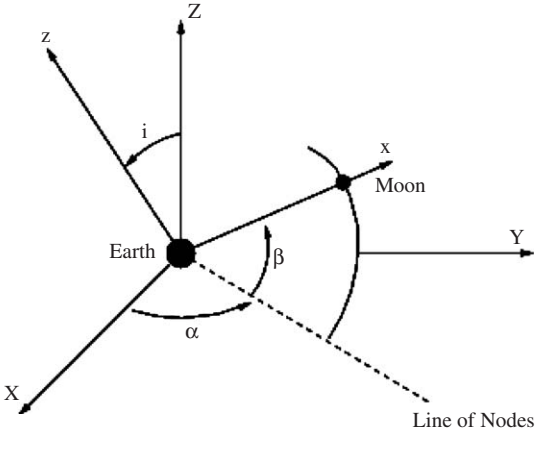

Fig. 1. Angle definitions; X, Y, and Z define the Sun–Earth rotating frame; x, y, and z are fixed in the Earth–Moon rotating frame.

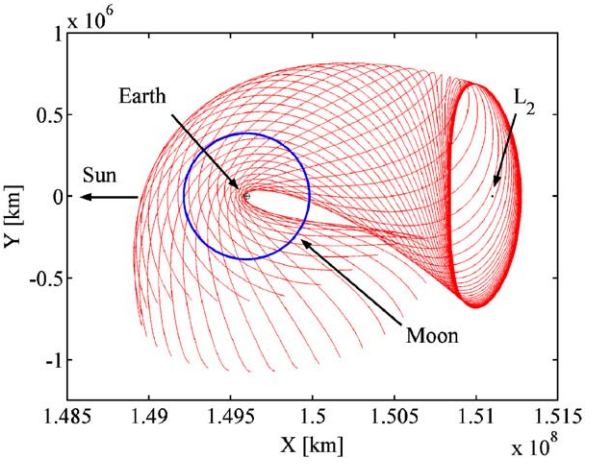

Fig. 2. Sun–Earth unstable manifolds near L_2; $Ay = 699,000$ km, $Az = 200,000$ km.

the Earth–Moon manifolds, thus, it is not necessary to compute them for potential system-to-system transfers. To tag manifolds along the tube that may be useful, the halo orbit is decomposed into four regions, A, B, C, and D, as seen in Fig. 3. In computation of manifolds by integration of specific sets of initial conditions, manifolds departing from regions C and D are accessible to Earth–Moon manifolds. Thus, the search is focused on this part of a Sun–Earth tube.

Stable and unstable manifolds also exist in the Earth–Moon system since periodic orbits can be computed near all collinear libration points. For instance, once a stable manifold tube for a specified halo orbit is

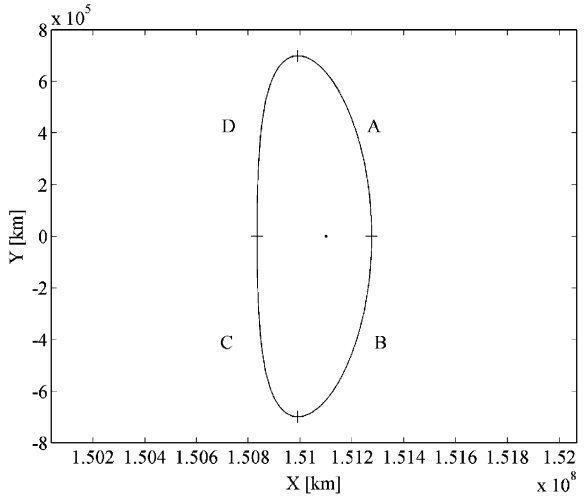

Fig. 3. Sun–Earth halo orbit near L_2; $Ay = 699,000$ km, $Az = 200,000$ km.

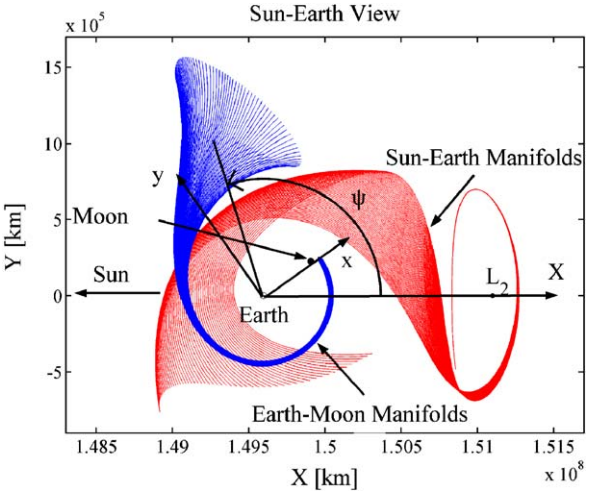

Fig. 4. Earth–Moon (EM) and Sun–Earth (SE) manifolds corresponding to the initial conditions: EM $Ay = 41,100$ km, EM $Az = 30,000$ km, SE $Ay = 699,000$ km, SE $Az = 200,000$ km.

propagated backwards in the Earth–Moon coordinate frame, the position and velocity states along the tube can be transformed to another frame for visualization. In Fig. 4, the relevant part of the Sun–Earth manifold is plotted in red. It is computed from regions C and D along the halo orbit. Also in the figure, the Earth–Moon stable manifold tube (blue) has been transformed to the Sun–Earth coordinate frame and plotted. The x- and y-axis appear in the figure to indicate the *initial* position of the Moon. The transformation in the figure assumes arbitrary values for the orientation of the Earth–Moon coordinate frame, that is, $\alpha = 60°$ and $\beta = -30°$.

3. System-to-system analysis

To successfully compute a system-to-system transfer requires a methodology that identifies the spatial intersection of the manifold tubes. Such a task is nontrivial. The methodology developed here, in the 3D problem, exploits projections of the phase space into lower dimensions that are then used for transfer trajectory design, similar to the applications of Poincaré sections in two dimensions.

3.1. Poincaré sections

In this simplified model, the key concept in the design of system-to-system transfers is that the manifold tubes in the phase space provide the "pathways" from one system to another and, thus, this basic structure controls the trajectory. The intersection of the tubes allows motion from one system to the next. Demonstrated by Koon et al. [8] in the 2D CR3BP, the intersection can be identified via Poincaré sections. In the 3D spatial CR3BP, the phase space is 6D; the Jacobi constant reduces it by one. Then, for some transversal slice, the Poincaré section is an object in 4D. The intersection of two such objects is not obvious. As discussed by Gómez et al. [11] however, projections of the objects onto lower dimensional planes can yield significant insight. Such projections originate with additional characteristics for the transfer that might be specified. For example, from the Sun–Earth halo orbit, integrate a tube associated with the unstable manifold forward in time until the trajectories cross the "PS" plane. This location is identified by the angle ψ in Fig. 5 that can be visualized in Fig. 4. The angle ψ is measured from the X-axis and specifies a plane for intersection of the tubes. The angle is positive for rotation counter-clockwise about the Z-axis. Once the angle ψ is specified, a stable manifold tube in the Earth–Moon system can be computed to

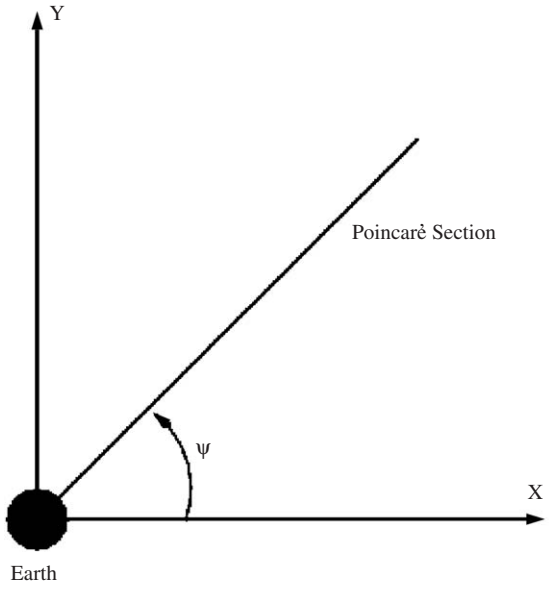

Fig. 5. Definition of ψ.

also arrive at the same PS plane in negative time. It is noted again that, in the spatial problem, this plane is not actually a Poincaré section, merely a projection given specified characteristics. It is denoted as a section for simplicity. Given that both manifold tubes are projected onto this plane and an intersection is determined, a transfer is defined by a search for essentially two possible types of state vectors. One type is a position state that is *on* both tubes (with a possible velocity discontinuity). A location on the tube (or, in reality, very near), ensures that the solution will pass from the Sun–Earth halo orbit to an Earth–Moon halo orbit. However, a transit orbit inside the tubes can also accomplish a shift from one system to the other. Transit orbits may or may not pass very close to the boundary. Since this study does not consider transitions from a stable to an unstable manifold corresponding to the same libration point orbit, nontransit orbits are not considered here.

From the general concept, defining a transfer via intersecting tubes, the lowest cost option is sought. But, the complexity of the system-to-system transfer problem between the Earth–Moon and the Sun–Earth systems increases further when the inclination of the lunar orbit is introduced. For efficient transfer design, the orientation of the Earth–Moon system, that is, the timing in the ephemeris model, is critical. The orientation of the Earth–Moon coordinate frame is determined by the three angles, α, i (fixed), and β. Of course, the location of the PS plane is another design parameter and unknown. Thus, the search for a low cost transfer is reduced to the three angles α, β, and ψ. It is necessary to search over the two angles α and β, as well as the PS plane orientation angle ψ.

3.2. Manifold intersections

In the spatial problem, the intersection of two manifold tubes is nontrivial. In an automated process, it is especially difficult without the benefit of any visual inspection. To aid in this process, once the PS plane is identified and a potential intersection exists, a new coordinate frame is defined in the physical PS plane. A Z_{ref}-axis is defined parallel to the Z-axis in the Sun–Earth system. Physically, the X_{ref}-axis is in the PS plane and oriented relative to the X-axis by the angle ψ. In this way, the position components along the Y_{ref}-axis are always zero.

Even though Earth–Moon manifolds and Sun–Earth manifolds form a continuous surface, they are usually computed numerically from individual trajectories. An example of intersecting Earth–Moon and Sun–Earth manifolds appears in Fig. 6, where discrete points are plotted in the PS plane. It is apparent that computation of the actual point of intersection, even in the physical plane of the figure, is nontrivial. Thus, an approximate method is required to determine the intersection in a short period of time. The intersection point is estimated in configuration space via splines. From the estimate, the full state vectors can be computed.

Although an intersection of the tubes in configuration space will yield a transfer, the velocity states are not generally equal and a maneuver is required. Most likely, the Earth–Moon and Sun–Earth manifolds

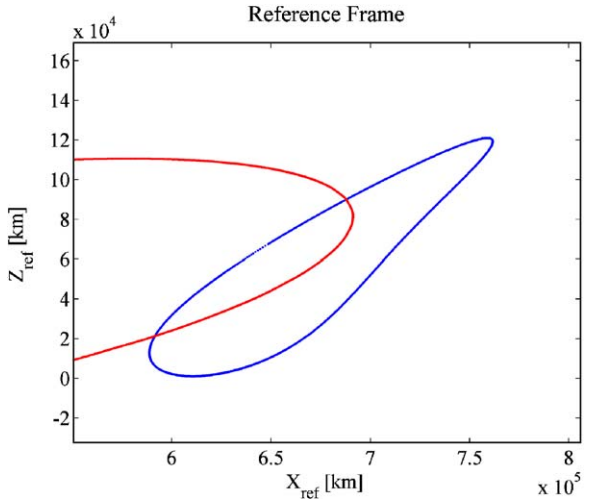

Fig. 6. EM manifolds (closed blue curve) and SE manifolds (open red curve) in the PS reference frame.

actually intersect in, at least, two points in the PS plane (see Fig. 6). It is simple to determine which of the two possesses a smaller velocity discontinuity. The point of interest, however, is undoubtedly not at the best orientation. Thus, a modification of α and β will improve the result. To change the orientation, without affecting the intersecting point, it is necessary to change α and β at the same time. For example, when α is increased, β is decreased by the same angle. Strictly speaking, the intersecting point changes because the Earth–Moon manifolds are inclined. But, incorporating this assumption renders a preliminary estimate of the angles that results in a reasonably low maneuver cost.

3.3. Transit orbits and maneuvers

To complete a transfer between the Earth–Moon and Sun–Earth systems, one option is to shift between trajectories that lie on the manifold surfaces. Generally, the velocity states are not equal at the intersection point and the ΔV is computed as the norm of the vector defined by the differences in the velocity components. However, a transit orbit will also deliver a vehicle between the systems. To determine a transit orbit, velocity components must satisfy certain conditions [7]. Again, projections onto the PS plane are useful in the form of phase plots of velocity components as functions of position components. Two phase plots for the Earth–Moon tube (blue) and Sun–Earth tube (red) appear in Fig. 7. The X_{ref} components are plotted on the left, and on the right are curves representing the relationship for Z_{ref} components. For the selected Sun–Earth manifolds, note that the curves do intersect. The closed blue curves are boundary conditions for a transit orbit [7]. Thus, when a maneuver is applied, the new velocity components must be within the blue boundaries to approach the Moon. Another condition for a transit orbit is the Jacobi constant. The value of the Jacobi constant corresponding to a transit orbit must equal the value for trajectories on the Earth–Moon tube. However, because of the transformation, the value of the Jacobi constant changes for points that lie on the blue Earth–Moon curve in Fig. 7, i.e., in the PS coordinates and Sun–Earth rotating frame. Thus, it is most efficient to first transform the curves from Fig. 7 into the Earth–Moon rotating frame. The value of the Jacobi constant along the Earth–Moon manifolds is constant for representations in the Earth–Moon rotating frame. When points that intersect the PS plane of the Sun–Earth frame are transformed into the Earth–Moon rotating frame, they are no longer contained in a plane, however. In this case, two phase plots are no longer sufficient to determine the boundary conditions. It is useful to define a new local "Poincaré section" and reference frame in the Earth–Moon rotating frame. The definition of the new reference frame appears in Fig. 8. The x_{ref}-axis is directed from the barycenter of the system to the tube intersection point of interest from Fig. 7. The z_{ref}-axis is parallel to the z-axis, and the y_{ref}-axis is perpendicular to the x_{ref}–z_{ref} plane. Thus, this new projection of the Poincaré section is defined by the x_{ref}–z_{ref} plane. The black solid line in Fig. 8 represents the x–y projection of the new PS_{EM} plane. Phase plots of Earth–Moon manifolds on the PS_{EM} appear in Fig. 9. These plots

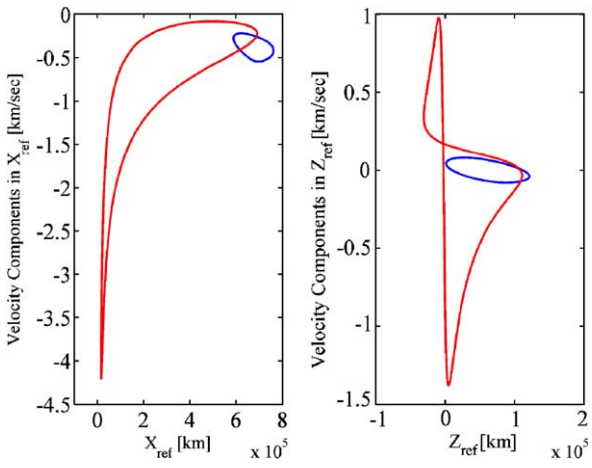

Fig. 7. Velocity vs. position at Poincaré section; Earth–Moon manifolds (small blue curve) and Sun–Earth manifolds (large red curve).

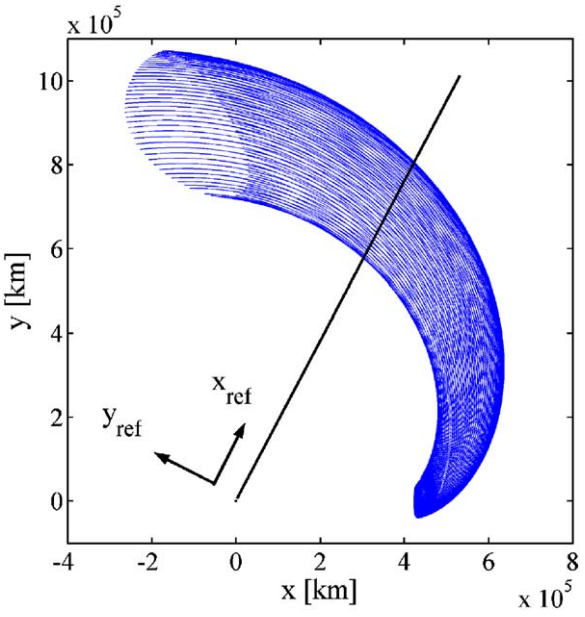

Fig. 8. New local PS_{EM} reference frame in Earth–Moon rotating frame.

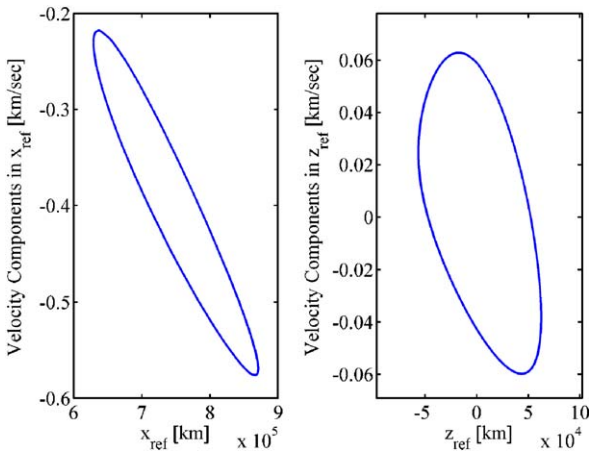

Fig. 9. Velocity vs. position in the PS_{EM} reference frame in Earth–Moon rotating frame; Earth–Moon manifolds.

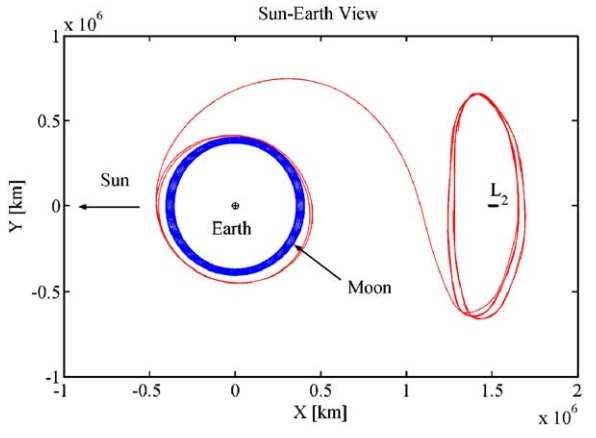

Fig. 10. Halo-to-halo transfer in the Sun–Earth rotating frame; initial guess from CR3BP: EM $Ay = 41,100$ km, EM $Az = 30,000$ km, SE $Ay = 699,000$ km, SE $Az = 200,000$ km.

relate velocity as a function of position in both the x_{ref} and z_{ref} components. Now, the maneuver can be computed with these two phase plots and the value of the Jacobi constant for the Earth–Moon tube.

3.4. Example: halo-to-halo transfer

A transfer from a Sun–Earth halo orbit to an Earth–Moon halo orbit in the CR3BP is most simply achieved by connecting invariant manifolds. The velocity difference between the Earth–Moon and a Sun–Earth manifold at the intersection point becomes the ΔV for the transfer. For example, consider a Sun–Earth L_2 halo orbit with $Az = 200,000$ km and an Earth–Moon L_2 halo orbit with $Az = 30,000$ km. The ΔV computed from the previous methodology is 22.2 m/s when ψ is arbitrarily selected to be 95°. To test the validity of this result, it is transitioned to the ephemeris model. The software package Generator, developed at Purdue University, is used to simulate the results in Fig. 10. A complete halo-to-halo transfer in the ephemeris model appears in Fig. 10. The figure is centered at the Earth and, in the Sun–Earth rotating frame, the Sun's direction is indicated. The ephemeris Moon location throughout the transfer appears in the figure in blue. A closeup of the transfer arriving in an Earth–Moon Lissajous orbit is plotted in Fig. 11. This figure is centered at the Moon. The Earth is placed to the left of the Moon for a reference, but it shifts position in an ephemeris model. The ephemeris results appear in Table 1. In the ephemeris model, this transfer can be achieved with zero ΔV. The sizes of the Earth–Moon and Sun–Earth Lissajous orbits are slightly different from the sizes of original halo orbits, i.e., now Earth–Moon $Az = 30,300$ and Sun–Earth $Az = 195,000$ km.

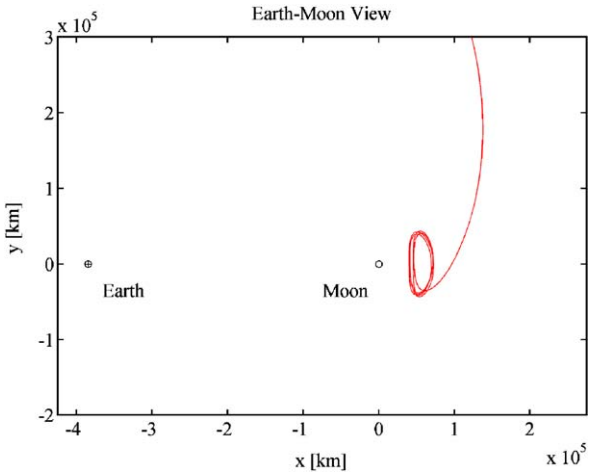

Fig. 11. Earth–Moon manifold asymptotically approaching an Earth–Moon Lissajous orbit.

Table 1
Transfer results in the ephemeris model

Earth–Moon Az (km)	Sun–Earth Az (km)	ΔV (m/s)
30,300	195,000	0

4. Results using manifold intersections

A large challenge in trajectory design in a multibody regime is the sensitivity. Nevertheless, a large

number of transfers can be determined using the previous design strategy. The results that emerge highlight some useful relationships, particularly the angle relationships that yield the results with the lowest cost. It was originally assumed that the key relationship to design transfers between the Earth–Moon and the Sun–Earth systems is the orientation of the Earth–Moon system in the Sun–Earth rotating frame. More information about the orientation of the Earth–Moon system reduces the computation time in the trajectory design process. Since the orientation is determined by α and β for a certain lunar phase angle ψ, any known relationship between these angles is useful.

4.1. Relationship between θ and ψ

First, it is necessary to examine which combinations of angles are related in a simple or straightforward manner. Since the angles α and β are traded off in the design process, their sum is notable and this angle is defined to be θ, i.e., $\theta = \alpha + \beta$. An example of the relationship between θ and ψ appears in Fig. 12. A particular Sun–Earth halo orbit with out-of-plane amplitude $Az = 200,000$ km is defined and transfers are computed to Earth–Moon halo orbits of various amplitudes. The range of the angle θ is selected from 80° and 110°. Usually, Earth–Moon and Sun–Earth manifolds intersect within this range. Fewer opportunities to obtain intersections exist beyond these values. The Earth–Moon orbits are sized from Az values of 16,000 to 30,000 km. The plots are not smooth because the angle increment is fixed at one degree. To achieve smoother

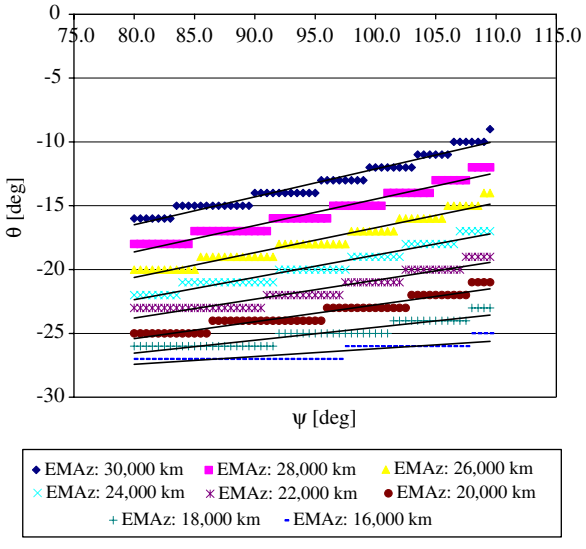

Fig. 12. Relationship between θ and ψ; SE $Az = 200,000$ km.

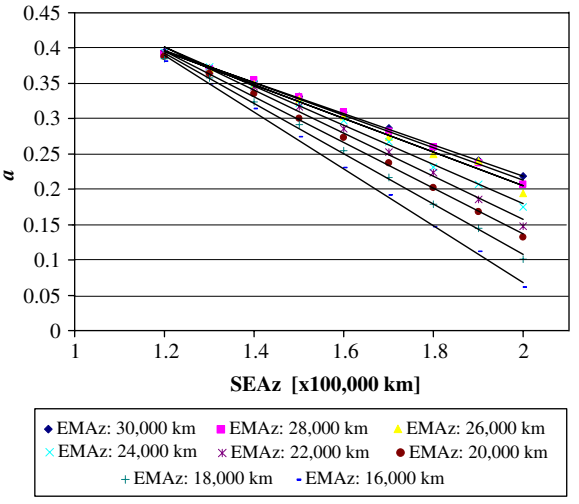

Fig. 13. Relationship between a and SE Az for each EM Az.

results, the increment could be reduced, for example, 0.1°. However, an increment of one degree is sufficient to observe trends. The solid lines are linear fits of each data set. Thus, θ and ψ appear linearly related for different Earth–Moon halo orbits paired with a Sun–Earth periodic orbit of $Az = 200,000$ km. This result is also true if a search for transfers is expanded to include other Sun–Earth periodic orbits with Az amplitudes from 120,000 to 200,000 km. Thus, it is possible to relate θ and ψ for each case by a linear equation i.e., $\theta = a\,\psi + b$. Moreover, these variables can be correlated in other ways. A linear relationship between the slope a and the Az amplitude of the Sun–Earth halo orbit appears in Fig. 13; transfers to various Earth–Moon halo orbits are included. The relationship between b and various Sun–Earth halo orbits (represented through their Az amplitude) appears in Fig. 14. Thus, these relationships allow an immediate estimate of θ for any lunar phase ψ and the correlation of these angles to the size of various Earth–Moon and Sun–Earth orbits. Although these relationships are very useful, the orientation of the Earth–Moon system is not immediately determined because θ is a combination of α and β. To determine a specific orientation, it is necessary to specify α or β. Once either angle is available, the other is obtained from θ.

4.2. Relationship between α and β

Given the value of θ, if the relationship between α and β is identified, the angles can be determined. The relationship between α and β actually appears to be somewhat nonlinear. The relationship for transfers from

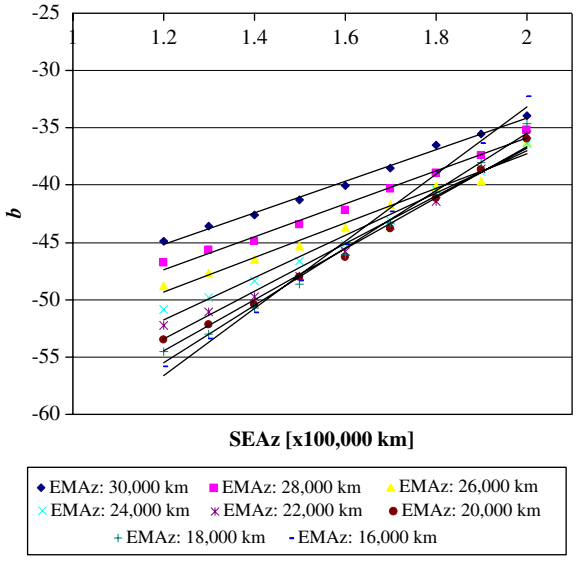

Fig. 14. Relationship between b and SE Az for each EM Az.

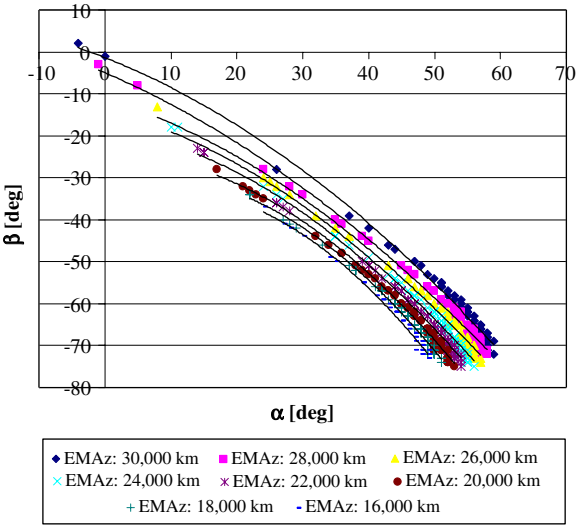

Fig. 15. Relationship between α and β for SE $Az = 120,000$ km; various EM Az orbits.

a Sun–Earth halo orbit of $Az = 120,000$ km appears in Fig. 15. The solid lines are quadratic fits of the data set. As the Az amplitude of the periodic Sun–Earth orbit is increased, the relationship becomes more complicated. Various transfers from a Sun–Earth halo orbit of $Az = 200,000$ km to a number of Earth–Moon orbits are plotted as points in Fig. 16. The data points are not in any obvious relationship. However, the points are crowded into certain regions. Thus, the general trends are identified from crude linear relationships. As seen

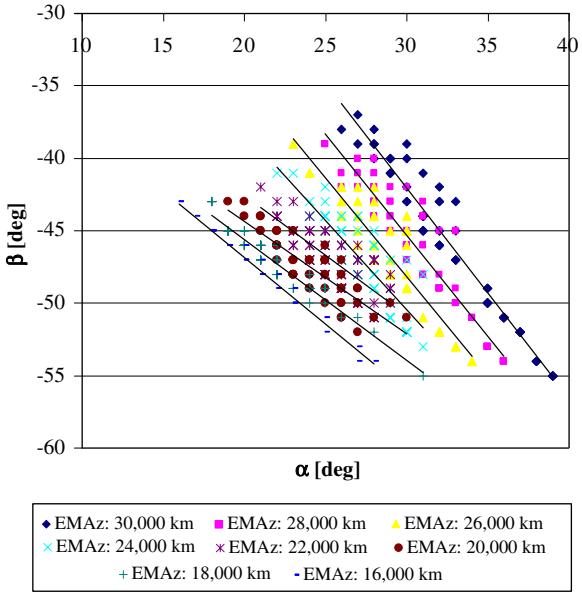

Fig. 16. Relationship between α and β for SE $Az = 200,000$ km; various EM Az orbits.

in the figure, the solid lines do not pass through all the data points. But, the combinations that appear in the figure offer initial estimates.

4.3. Transfers: α–β combinations

Even though the relationship between α and β is not known perfectly, it is now possible to estimate the values of α and β that will yield a successful system-to-system transfer for each combination of Earth–Moon and Sun–Earth halo orbits. Results using the α–β estimated relationship are compared with actual data in Table 2. For this case, the Earth–Moon orbit is defined such that $Az = 30,000$ km and the corresponding Sun–Earth halo possesses $Az = 200,000$ km. Also, note that ψ is selected to be 95°. From such an initial transfer, the cost is investigated to determine: (a) whether the transfer can be transitioned to the ephemeris model and (b) whether a lower cost transfer can be computed from the estimate, if necessary. If the results are satisfactory, the estimate is useful. Some results are compared in Table 3. In the CR3BP, a transfer is constructed using the α–β estimated relationship to determine the orientation of the Moon at initiation of the transfer. The resulting ΔV for a manifold-to-manifold transfer is 20.7 m/s. This value is actually smaller than a nearby transfer computed as part of the initial sweep of solutions, a maneuver equal to 22.2 m/s. More importantly, the final results in the ephemeris model are

Table 2
Angles α and β computed from actual data and the estimated relationship; EM $Az = 30,000$ km, SE $Az = 200,000$ km, $\psi = 95°$

	α (deg)	β (deg)
Actual data	31	−45
Estimate	33	−46

Table 3
Comparison of results from the original data and the estimated relationship; EM $Az = 30,000$ km, SE $Az = 200,000$ km

	Data	Estimate
CR3BP		
ΔV (m/s)	22.2	20.7
Ephemeris		
EM Az (km)	30,300	30,900
SE Az (km)	195,000	197,000
ΔV (m/s)	0	0

Table 4
Comparison of α and β from the original data and estimated relationship; EM $Az = 30,000$ km

Sun–Earth Az (km)	Data		Estimate	
	α (deg)	β (deg)	α (deg)	β (deg)
190,000	35	−48	35	−48
180,000	38	−50	37	−49
170,000	43	−55	38	−50
160,000	47	−58	44	−54
150,000	49	−59	47	−57
140,000	51	−60	50	−59

nearby solutions, and in both cases, the ΔV is reduced to zero. Thus, a slight difference in the α–β angles did not significantly affect the final result and the estimate is satisfactory.

Other examples appear in Table 4. All cases share the same phase angle, $\psi = 95°$, and the Earth–Moon halo orbit with $Az = 30,000$ km. The largest difference between the original data and the estimated angles is noted for the Sun–Earth orbit of $Az = 170,000$ km. The difference is 5° for each angle. However, once the $Az = 170,000$ km case from Table 4 is transitioned to the ephemeris model, a zero cost solution still emerges from both CR3BP transfers. The comparison of the results in the ephemeris model appears in Table 5. Thus, even though the ΔV computed from the angle relationship is slightly larger in the CR3BP, the out-of-plane Az amplitude in the final Lissajous orbits in the ephemeris model are still close to those specified in the CR3BP.

Table 5
Comparison of results from estimated relationship and original data; EM $Az = 30,000$ km, SE $Az = 170,000$ km

	Data	Estimate
CR3BP		
ΔV (m/s)	14.0	23.1
Ephemeris		
EM Az (km)	25,900	26,400
SE Az (km)	167,000	169,000
ΔV (m/s)	0	0

Such results are useful in the design process. That is, nearby solutions are available for different α–β combinations.

4.4. Transfers: Sun–Earth/Earth–Moon halo orbit combinations

The methodology allows for the computation of relatively low cost system-to-system transfers in a short time. Thus, it is possible to collect a large amount of data for a variety of cases. A comparison of interest is the combinations of Earth–Moon and Sun–Earth halo orbits that yield the lowest cost transfers. The halo orbits are always represented by their out-of-plane amplitude, Az. The range of the Az amplitude for the Earth–Moon halo orbits covers 16,000 to 30,000 km. The Sun–Earth periodic orbits range over values of Az from 120,000 to 200,000 km. Also, the angle ψ varies from 80° to 120°. The best result for arrival into each Earth–Moon halo orbit appears in Table 6. From the results, good locations for maneuvers to achieve low cost transfers are apparently near $\psi = 110°$, except in the last case. Also, for all Earth–Moon halo orbits, it appears possible to achieve a transfer with a relatively small ΔV.

To obtain complete information, it is necessary to examine the results in the ephemeris model. All results in Table 6 are transitioned to the ephemeris model, and the results appear in Table 7. The Earth–Moon halo orbits are fixed at the original values in terms of amplitude. Then, a Lissajous-to-Lissajous transfer is constructed by applying the same ΔV that is obtained in the CR3BP. If necessary, the Sun–Earth halo orbit is modified via a change in the amplitude Az. For each combination, a transfer is accomplished successfully with a change in the Sun–Earth orbit. The transfer to an Earth–Moon orbit with $Az = 18,000$ km requires a ΔV of 10.6 m/s. This value is actually less than that computed in the CR3BP. Note that further reduction in the ΔV can be accomplished in the ephemeris model if

Table 6
Best Sun–Earth Az and ψ combinations for each EM Az; halo-to-halo transfer

Earth–Moon Az (km)	Sun–Earth Az (km)	ΔV (m/s)	ψ (deg)
16,000	120,000	17.9	110.5
18,000	130,000	14.5	109
20,000	130,000	11.0	110
22,000	130,000	7.5	110.5
24,000	130,000	4.2	111
26,000	130,000	1.0	110
28,000	160,000	1.4	107.5
30,000	180,000	2.8	98

Table 7
Best combinations tested in the ephemeris model; Earth–Moon Az's fixed

Earth–Moon Az (km)	Sun–Earth Az (km)	ΔV (m/s)
16,000	113,000	17.9
18,000	133,000	10.6
20,000	161,000	11.0
22,000	115,000	7.5
24,000	124,000	4.2
26,000	129,000	0.9
28,000	154,000	1.4
30,000	155,000	2.8

Table 8
Best combinations with $\Delta V = 0$ m/s; the ephemeris model

Earth–Moon Az (km)	Sun–Earth Az (km)	ΔV (m/s)
16,000	111,000	0
18,000	142,000	0
19,000	140,000	0
22,000	126,000	0
24,000	130,000	0
26,000	131,000	0
28,000	155,000	0
30,000	157,000	0

there are no constraints. In fact, all can be reduced to zero for some change in the Sun–Earth Lissajous orbit. Transfers with zero ΔV appear in Table 8. Note that the Earth–Moon orbit in the third case changes from $Az = 20,000$ to $19,000$ km. To accomplish this result is more challenging than any other example. A change in only the Sun–Earth orbit is not sufficient. If flexibility exists to modify the size of the Earth–Moon orbit via the out-of-plane component, the zero cost transfer is computed. If the size of the Sun–Earth orbits is fixed, a zero cost transfer can also be accomplished by modification of the size of the Earth–Moon orbit in all cases. Actually, this option is easier to accomplish in general. However, since the magnitude of the Earth–Moon Az amplitude is smaller than that of the Sun–Earth orbit, the same amount of change in the Earth–Moon Az amplitude causes a larger percentage error. Thus, this option might not be desirable for certain missions.

5. System-to-system transfers from cells

System-to-system transfers computed using the previous design process rely on knowledge of the libration point orbits at each end of the transfer. The trajectory arcs are extracted directly from the invariant manifolds. However, that step is not necessary. For example, the particular libration point orbit may not be constrained or, in the case of transit orbits, the trajectory arc is not from a manifold. An alternative technique to compute a transfer involves the use of cells to represent a volume of manifolds [13]. This technique allows storage of a large amount of estimated manifold information in the CR3BP. Thus, it avoids computation of manifolds numerically for a wide variety of different periodic halo orbits to search for intersections. The halo orbit is a design parameter and emerges as part of the procedure.

Given a number of Sun–Earth L_2 periodic halo orbits, a set of cells can be created that approximates a continuous distribution of manifolds from the volume of halo orbits. Such a set of cells appears in Fig. 17; they approximate the stable manifolds corresponding to a range of L_2 halo orbits. Assume that some trajectory enters the volume. The trajectory may be an Earth–Moon manifold, an Earth–Moon transit orbit, or some other

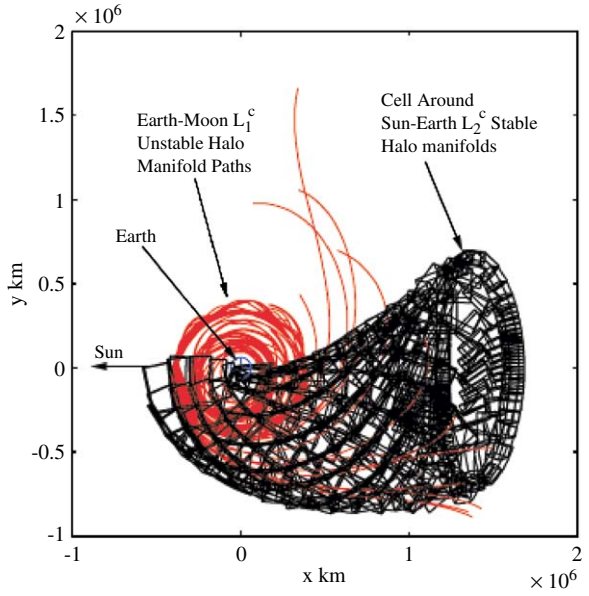

Fig. 17. EM manifolds intersect cells.

Table 9
Results from the cell estimation technique; CR3BP

Earth–Moon Az (km)	30,000
Sun–Earth Az (km)	165,000
ψ (deg)	123.9
ΔV_1 (m/s)	14.4
ΔV_2 (m/s)	7.6

Table 10
Results with zero cost in ephemeris model

Earth–Moon Az (km)	29,000
Sun–Earth Az (km)	160,000
ΔV_1 (m/s)	0
ΔV_2 (m/s)	0

trajectory from another region of space. In the figure, the unstable manifolds associated with an Earth–Moon L_1 halo orbit of amplitude $Az = 39,000$ km are entering the volume. The goal is to deliver the trajectory to the region of the Sun–Earth L_2 libration point orbit with a minimum cost. For any trajectory that enters the volume, a cell can be identified that envelops the entering trajectory. Within the cell, approximate analytical relationships represent position and velocity states for manifolds that approach Sun–Earth L_2 halo orbits. A maneuver to bring the trajectory to a halo orbit can be approximated. Transitioned to the ephemeris model, an actual transfer can be determined and the cost reduced, frequently to zero [13]. In this example, only the manifolds in the Sun–Earth system have been approximated, but approximations for the Earth–Moon system are also possible.

For this investigation, the problem is focused on transfers from Sun–Earth L_2 halo orbits to the vicinity of the Moon. Let an Earth–Moon halo orbit be defined by an Az amplitude of 30,000 km. From the numerical study summarized in Table 6, the "best" Sun–Earth halo orbit for this transfer is $Az = 180,000$ km. Recall that the ΔV is equal to 2.8 m/s at a phase angle $\psi = 98°$. The orientation of the Earth–Moon tube is determined such that $\alpha = 31°$ and $\beta = -44°$. Then, this Earth–Moon tube is propagated to enter the cell volume. A search ensues for an intersecting Sun–Earth manifold that yields the lowest ΔV. For a single Earth–Moon manifold, all the intersecting Sun–Earth manifolds in the local volume are examined. The results from the cell estimation process in the CR3BP appear in Table 9. The Sun–Earth Az is reduced to 165,000 km. Also, the resulting value of ψ is 123.9°. This is beyond of the range of the ψ angle that is typically examined (80–120°) in this study. The manifold intersection process will still determine an intersection at this value of ψ using the same orientation angles. However, the ΔV values are usually larger with ψ beyond the typical range. Actually, in this case, the manifold intersection process yields $\Delta V = 60.6$ m/s at $\psi = 123.9°$ for the same orientation. However, the transfer estimation process using cells incorporates two ΔVs. The first, ΔV_1, is a maneuver to leave a Sun–Earth halo orbit. This maneuver is required because the cell estimation technique uses the estimation of manifolds, not actual, globalized manifolds. The second maneuver, ΔV_2, is the maneuver to transfer from a Sun–Earth manifold to an Earth–Moon manifold. Thus, the total ΔV is the sum, i.e., 22.0 m/s. The approximation from the cell procedure is also shifted to the ephemeris model and can, once again, be reduced to a system-to-system transfer with zero cost. The results in the ephemeris model appear in Table 10. The final solution, based on an initial guess with two maneuvers, is different than that obtained from the angle approximations. A solution still exists, however.

6. Transfer from Sun–Earth halo orbit near L_2 to the Moon

The accessibility of the Moon may also be critical in the system-to-system design problem. Computation of a transfer from a halo orbit in the Sun–Earth L_2 family to a lunar orbit is also possible by using this system-to-system transfer design strategy, i.e., halo-to-halo transfers and transfers incorporating transit orbits.

6.1. Halo-to-halo transfer

A straightforward option to reach the Moon from a halo orbit near the Sun–Earth L_2 libration point is a simple modification of a halo-to-halo transfer. Since a halo-to-halo transfer allows arrival in the vicinity of an L_2 halo orbit in the Earth–Moon system, the transfer to the Moon can be accomplished by exploiting an unstable Earth–Moon manifold after arrival in the Earth–Moon libration point orbit. One example in the ephemeris model appears in Fig. 18. The original halo-to-halo transfer in the CR3BP between a Sun–Earth halo orbit of amplitude $Az = 130,000$ km and arrival in an Earth–Moon halo orbit with Az equal to 24,000 km is selected for this example. With this combination, the Earth–Moon Az amplitude and Sun–Earth out-of-plane Az do not change as the solution is shifted to the ephemeris model as is evident in Table 8. The Lissajous-to-Lissajous trajectory in Fig. 18 is plotted

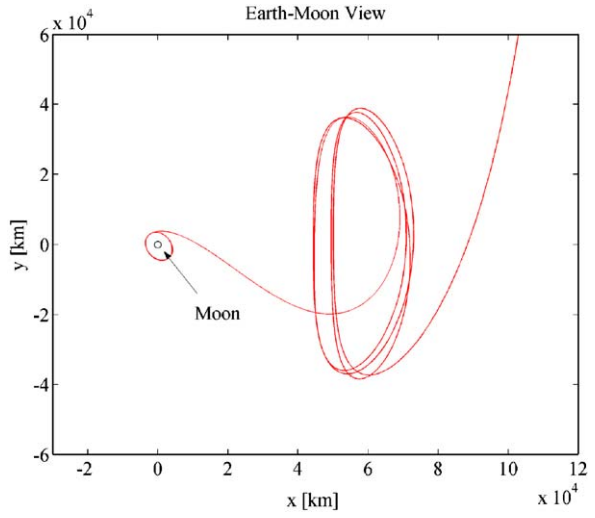

Fig. 18. Arriving at the Moon via halo-to-Moon transfer; Earth–Moon rotating frame; Earth–Moon $Az = 24,000$ km; ephemeris model.

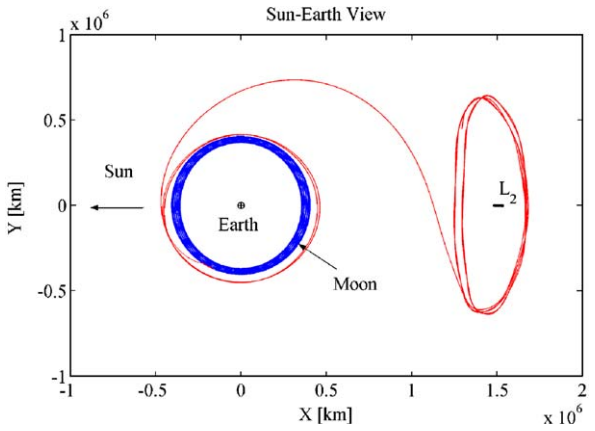

Fig. 19. Lissajous-to-Moon transfer in the Sun–Earth rotating frame; ephemeris model.

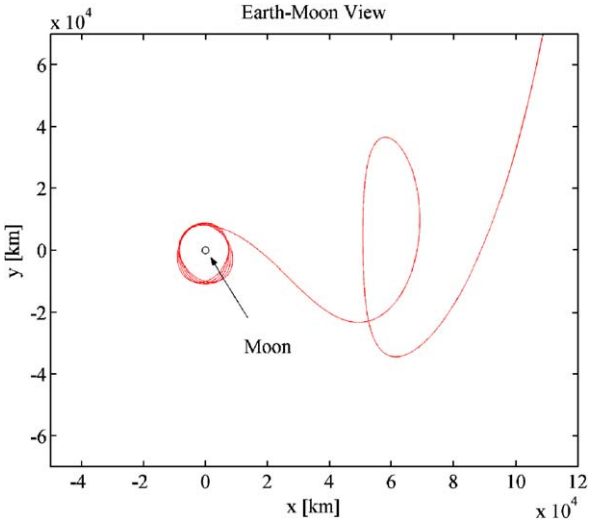

Fig. 20. Transfer to the Moon via a transit orbit; Earth–Moon $Az = 24,000$ km; ephemeris model.

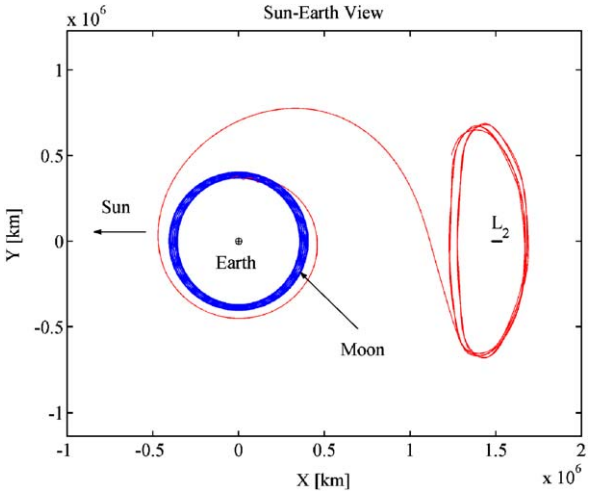

Fig. 21. Lissajous-to-Moon transfer in the Sun–Earth rotating frame; ephemeris model.

in the Earth–Moon rotating frame. Departure from a halo or Lissajous along an unstable manifold incurs no cost. The trajectory includes at least one revolution of the Moon. A maneuver is necessary, of course, to maintain the lunar orbit. In this example, the altitudes at the periapsis and apoapsis of the new orbit are 2090 and 3230 km. Also noted, the angle between the orbit plane and the Earth–Moon x–y plane is about 35°. The end-to-end transfer from the Sun–Earth L_2 Lissajous orbit to a Moon orbit in the Sun–Earth rotating frame as computed in the ephemeris model appears in Fig. 19.

6.2. Transit orbit

A system-to-system transfer can also be accomplished by computing a transit orbit inside a stable Earth–Moon tube. Transit orbits allow a more direct delivery of the trajectory to the vicinity of the Moon. Thus, it is possible to apply transit orbits in developing transfers to the Moon. An example of such a transfer in the ephemeris model appears in Figs. 20 and 21. The sizes of these orbits are the same as those in the previous example. The arrival orbit does not converge to the halo orbit, but rather approaches the Moon. Again, this

transfer is cost-free to the vicinity of the Moon and the trajectory encircles the Moon at least once. Then, a ΔV is, of course, necessary to permanently insert into lunar orbit. In the figure, the periapsis and apoapsis of this new orbit are 6980 and 9170 km, respectively. Also, in this example, the angle between the orbit plane and the Earth–Moon x–y plane is about 21°. No constraint was applied to specify a particular inclination. A complete transfer in the Sun–Earth rotating frame appears in Fig. 21.

7. Summary

The objective of this research effort is the development of a technique for the preliminary design of system-to-system transfers between the Sun–Earth and Earth–Moon systems. The technique is based on the application of the dynamical structure of the invariant manifold tubes associated with the periodic libration point orbits. This technique allows a search for low cost transfers in a relatively short time period by limiting the search space with the knowledge of the dynamics. The linear and quadratic angle relationships are introduced to determine desirable orientations of the Earth–Moon system for low cost transfers. These relationships can directly determine an orientation of the Earth–Moon system in the Sun–Earth rotating frame for orbit sizes and the lunar phase angle ψ, within certain error bounds. The relationships then represent timing constraints in the full model. All results are successfully reproduced in the ephemeris model for zero cost and meet all timing conditions. Examples of transfers to the Moon are introduced by application of the process to construct a halo-to-Moon transfer via a Lissajous or transit trajectory. These transfers allow a relatively quick design process for transferring from a Sun–Earth Lissajous orbit near L_2 to the vicinity of the Moon for zero cost. Although the transfers summarized here are only one-way, i.e., the Sun–Earth system to the Earth–Moon system, this technique can be modified for various types of transfers between two systems.

Acknowledgements

The authors are grateful to Purdue University for continuing support of this project. Christopher Patterson, from Purdue University, is also acknowledged for the results using the cell estimation technique.

References

[1] R.W. Farquhar, D.W. Dunham, Y. Guo, J.V. McAdams, Utilization of libration points for human exploration in the Sun–Earth–Moon system and beyond. Acta Astronautica 55 (2004) 687–700.

[2] D.C. Folta, M. Beckman, S.J. Leete, G.C. Marr, M. Mesarch, S. Cooley, Servicing and deployment of national resources in Sun–Earth libration point orbits, in: 53rd International Astronautical Congress, The World Space Congress, Houston, Texas, October 2002, Paper IAC-02-Q.6.08.

[3] M.W. Lo, S.D. Ross, The lunar L_1 gateway: portal to the stars and beyond, in: AIAA Space Conference and Exposition, Albuquerque, New Mexico, August 2001.

[4] K.C. Howell, B.G. Marchand, M.W. Lo, Temporary satellite capture of short-period Jupiter family comets from the perspective of dynamical systems, Journal of the Astronautical Sciences 49 (4) (2001) 539–557.

[5] M.W. Lo, The interplanetary superhighway and the origins program, in: IEEE Aerospace Conference Proceedings, vol. 7, 9–16, March 2002, pp. 3543–3562.

[6] F. Topputo, M. Vasile, A.E. Finzi, An approach to the design of low energy interplanetary transfers exploiting invariant manifolds of the restricted three-body problem, in: 14th AAS/AIAA Space Flight Mechanics Conference, Maui, Hawaii, February 2004, Paper No. AAS 04-245.

[7] W.S. Koon, M.W. Lo, J.E. Marsden, S.D. Ross, Shoot the Moon, in: AAS/AIAA Space Flight Mechanics Meeting, Clearwater, Florida, January 2000, Paper No. AAS 00-166.

[8] W.S. Koon, M.W. Lo, J.E. Marsden, S. Ross, Low energy transfer to the Moon, Celestial Mechanics and Dynamical Astronomy 81 (2001) 63–73.

[9] G. Gómez, W.S. Koon, M.W. Lo, J.E. Marsden, J. Masdemont, S.D. Ross, Connecting orbits and invariant manifolds in the spatial three-body problem, Nonlinearity, 2001.

[10] W. Koon, M. Lo, J. Marsden, S. Ross, Constructing a low energy transfer between Jovian moons, Contemporary Mathematics 292 (2002) 129–145.

[11] G. Gómez, W.S. Koon, M.W. Lo, J.E. Marsden, J. Masdemont, S.D. Ross, Invariant Manifolds, the Spatial Three-Body Problem and Space Mission Design, 2001, Paper No. AAS 01-301.

[12] J.S. Parker, M.W. Lo, Shoot the Moon 3D, in: AAS/AIAA Astrodynamics Specialists Conference, Lake Tahoe, California, August 2005, Paper No. AAS 05-383.

[13] K. Howell, M. Beckman, C. Patterson, D. Folta, Representations of invariant manifolds for applications in three-body systems, in: AAS/AIAA Space Flight Mechanics Conference, Maui, Hawaii, February 2004, Paper No. AAS 04-287.